Chapter 7

Vortex Methods

During the last few decades, the availability of powerful computers has resulted in a completely new branch of fluid mechanics: computational fluid dynamics (CFD). Today, CFD has become an enormously broad field of research in which a great diversity of numerical techniques is used. Vortex methods form one part of this field and several widely differing examples have been introduced in fluid mechanics literature. In this chapter we consider general set-up of 3-D vortex methods, some of the requirements they should satisfy, and some of the pros and cons of some vortex methods. We also give a short survey of some classes of methods in order to point out several drawbacks of existent vortex methods [1].

7.1 General Set-up of Vortex Methods

Vortex methods are computational methods aimed at the simulation of fluid flows by following the evolution of their vorticity field. The vortical structures in the flow field are represented by so-called vortex elements whose behaviour follows from solving their dynamic equations numerically.

The existence of vortex methods is related to the fact that fluid flows can be described by means of equations like the Helmholtz equation (2.2). The use of this vorticity formulation of the hydrodynamical equations has several important advantages above other formulations, e.g. the velocity-pressure formulation of the classical Euler equation [2]:

- vorticity, contrary to e.g. velocity, is frequently localized in space; consequently the amount of computational elements to be taken into account can be kept relatively small [3];
- according to Helmholtz's second theorem, vorticity behaves materially; consequently a Lagrangian approach is attractive, i.e. we can follow the vorticity field by tracking vortex structures which move along with the flow;
- since reconnection and intermittency in turbulence (see §§B and C of the Interlude) occur randomly in space and time, these phenomena are hard to investigate experimentally or by means of direct numerical simulation (DNS); simulations by means of vortex methods may be more appropriate.

Besides these general incentives to use vortex methods, in case of turbulent flows the generally recognized importance of coherent structures and their presumed relation with vorticity (see §B of the Interlude) has been another important motivation for the use of vortex methods.

[1] For a general review of vortex methods, see e.g. [121] and [207].

[2] Notice that the Helmholtz equation (2.2) can directly be obtained from the Euler equation by applying the "curl"-operator.

[3] Related to the above characteristic of the vorticity field, it has been thought that, though fluid motion itself has an infinite number of degrees of freedom, a study of vorticity fields may only require a finite number.

The general set-up of every vortex method follows from answering the following three questions:

1. **How do we discretize the vorticity field? or: What are the vortex elements?**

   Several vortex elements have been proposed, both of infinitesimal and finite dimensions. The simplest elements are vortex points, which just have a location and a strength. The so-called vortex blobs (or smoothed vortex points) are characterized by additional **smoothing functions** which determine the (variable) shape and size of the vorticity distribution in these elements. Another element is the vortex filament (see the definition in Chapter 2), which is determined by its location, torsion and curvature, and by its strength. Again, like vortex points, vortex filaments can be smoothed.

2. **Which equations for displacement and deformation of vorticity do we use and how do we transform these equations into equations for the chosen vortex elements?**

   For the calculation of the displacement of the vortex elements, the following expression may be applied:

   $$\frac{D\boldsymbol{x}}{Dt} = \boldsymbol{v}(\boldsymbol{x}, t) \tag{7.1}$$

   where $\boldsymbol{x}$ is the location vector and $\boldsymbol{v}$ the velocity vector at this location.

   The velocity field can be derived from the vorticity field according to the rule of Biot-Savart (2.3). However, application of this rule may require a method to avoid the singularity in the kernel of this integral equation (so-called regularization). In case of smoothed vortex elements, this problem is avoided as a result of the finite "core" size. Another approach is the so-called cut-off of the integration interval of the rule of Biot-Savart [4].

   The deformation (rotation and stretching) of vorticity can be described by either the Cauchy vorticity formula (1.4) or the Helmholtz equation (2.2). The first is generally applied in Lagrangian methods (defined above). The second are used in so-called Eulerian methods, i.e. methods in which the vorticity is regarded at fixed locations in the flow.

3. **How do we solve these equations numerically?**

   The numerical scheme will depend on the choice of the vortex elements, the deformation equations, the required accuracy and computational speed, etc. Therefore, no general recommandations can be given on this issue.

7.2 Vortex Method Requirements

A *reasonable* [5] vortex method as to meet several requirements. Some, in our view indisputable, requirements are given in this section; their order conveys our opinion about their relative importance [6].

[4] See [121] for a review. The cut-off technique was already applied in Thomson's 1883 *Treatise* [205, §11.1].

[5] It may be clear that discussion of the meaning of *reasonable* vortex methods is difficult. It strongly depends on the intention one has in mind applying a specific vortex method. Unfortunately, most authors working with vortex methods avoid a discussion of their intentions and of the applicability of their methods.

[6] One might argue that an additional, important, requirement should be added, i.e. no undesirable effects should be caused by the numerical scheme. One example of these effects is the influence of numerical or artificial viscosity. However, Beale & Majda [22] and Engquist & Hou in [9] have stated that vortex methods contain no inherent errors which act like the numerical viscosity of conventional Eulerian difference methods. Other requirements, like correct timestep adaption, are regarded as trivial and not typically related to vortex methods.

1. **divergence-free vorticity field**

   In an inviscid flow, the net flux of vorticity normal to the surface of any closed volume V, given by by $\int_{\partial V} \boldsymbol{w} \cdot \boldsymbol{n}$, should be zero. This requirement can be translated into: the vorticity field should be divergence-free, i.e.

   $$\nabla \cdot \boldsymbol{w} = 0 \tag{7.2}$$

   and is directly satisfied by a flow in which the relation (1.1) is preserved. Since this relation is the foundation of vorticity theory, this requirement is of significant importance.

2. **correct modelling of continuous distributions of vorticity**

   The vortex elements chosen for a vortex method have to provide a sufficiently accurate representation of continuous structures, like vortex rings. In general, one would like a representation which shows as many similarities in physical behaviour as possible compared with their "real" counterparts. However, this may not always be necessary or possible [7].

3. **correct representation of deformation and interaction of vortex structures**

   A correct modelling of vortex structures is no guarantee that the deformation (e.g. stretching, core deformation, stability) of vortex structures and the interaction of two or more of them (e.g. reconnection, alignment) will be correctly simulated. Comparison with experimental results is necessary to decide on this issue.

4. **conservation of motion-invariants**

   For inviscid vortex methods, the conservation of so-called motion-invariants should be satisfied. For 3-D vortex flows, the relevant invariants are total vorticity, total linear momentum, total angular momentum, total kinetic energy, and total helicity.

   Some authors (see e.g. [206]) have stated that this requirement can be reformulated as: the vorticity representation should be a weak solution of the equation describing vortex deformation. E.g., a weak solution of the Helmholtz equation has to satisfy the condition:

   $$\int f(\boldsymbol{x}) \{\frac{D\boldsymbol{w}}{Dt} - (\boldsymbol{w} \cdot \nabla)\boldsymbol{v}\} = \boldsymbol{0} \tag{7.3}$$

   for any so-called (smooth) test-function $f(\boldsymbol{x})$.

   A related requirement is conservation of the circulation (Kelvin's Circulation Theorem; see §4.1) of any closed vortex structure, e.g. a vortex ring.

5. **no negative effects of remeshing**

   Vortex methods may allow regions with fine-scale structures to develop in an intermittent manner. Nevertheless, remeshing may be required when lack of resolution arises. Care should be taken that the remeshing scheme (changing the time and/or space step in numerical simulations) involved in any vortex method should not introduce undesirable effects, which have no physical meaning or are forbidden from a physical point of view.

[7] In the Epilogue, some additional remarks on modelling can be found.

6. **correct boundary conditions**

   Boundary conditions should be imposed correctly. For vortex methods, free-slip conditions (i.e. zero velocity normal to the wall) may be imposed relatively easily by means of "mirrored" vorticity indicated by $\boldsymbol{w}^*$; see fig.7.1. However, the application of the

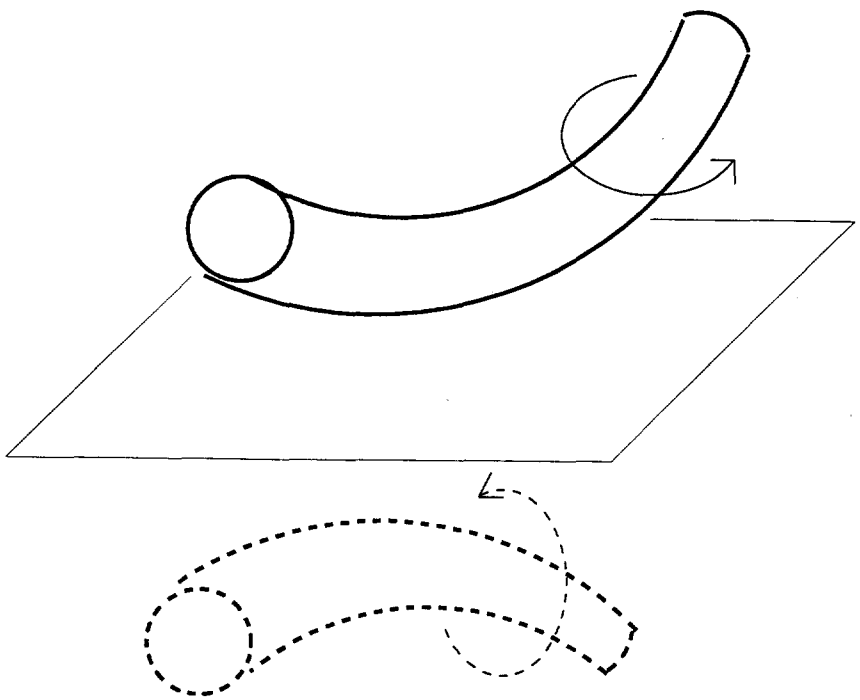

Figure 7.1: Imposing a free-slip boundary condition by addition of "mirrored" vorticity.

   no-slip condition (i.e. zero tangential velocity at the wall as required in viscous flows) usually requires much more care and effort.

7. **convergence**

   The requirement of convergence is related to the question: does the approximate solution obtained from the vortex method approach the exact solution? Convergence has been investigated both analytically and numerically for several vortex methods [8].

8. **acceptable computational effort**

   Though one of the attractions of vortex methods is the fact that computational points (vortex elements) are only required in rotational parts of the flow, the computation time is roughly proportional to the square of the number of vortex elements or coordinates. A Lagrangian method takes much computation time (usually claimed to be proportional to N^2, where N is the number of vortex elements). On the other hand, in an Eulerian approach, also parts of the flow field have to be regarded which may be insignificant.

[8] See Caflisch in [32] for a short survey of the issue of convergence. Anderson & Greengard [8] have pointed out that an investigation of the convergence of the numerical method used in the application of a vortex method should also be investigated. A more detailed discussion of convergence in case of vortex methods is postponed to §11.1.7.

7.3 A Short Survey of Vortex Methods

It is not easy to provide a fairly clear, short, and general survey of the vortex methods, which have been introduced and applied in the last few decades. The conceptual questions on vortex methods treated in §7.1 allow the division into several classes, though alternatives to our method of categorization may be proposed. Below, we will give a short survey of some inviscid, mainly 3-D, vortex methods. This survey is only intended to give an impression of the "state of the art".

7.3.1 Vortex-Filament Methods

In these methods, the elements are vortex filaments represented by 3-D curves, on which points are defined. In the so-called thin-filament method the core of the filaments is supposed to remain nearly constant in time and the wavelengths of disturbances along the filament are supposed to be much larger than the core radius. This vortex-filament method converges without smoothing, as is claimed in [90].

However, both assumptions mentioned above are not sufficient for accurate approximations of vortex motion [121] [9]. Therefore, smoothed-vortex-filament methods have been proposed. However, a parameter has to be chosen for these methods to get an appropriately averaged velocity of a collection of vortex lines. This leads to different schemes and to a dependence of conservation of e.g. energy on this parameter [121, p. 539].

In vortex-filament methods, the rule of Biot-Savart is applied to calculate the evolution of the space curves. No account is taken of the deformation of the vorticity field.

7.3.2 Vortex-in-Cell Methods

A rather different method is the vortex-in-cell method. Although the vorticity field is treated in a Lagrangian way, the Poisson equation for the streamfunction is solved on an Eulerian mesh to obtain the velocity field. It appears that because of the errors involved in this method, the simulations are sensitive to the size of the mesh, the number of vortices, the time-step, etc. Besides, they require relatively much computational effort. Artificial viscosity is introduced by the numerical scheme which makes this actually a viscous vortex method. For details we refer to e.g. [122, §4] and [207, §2.6].

7.3.3 Vortex-Point Methods

The oldest and perhaps best-known example of the vortex-point methods is the 2-D Lagrangian unsmoothed vortex-point method, which is better known as the point-vortex method (mentioned in the Interlude; see also [122, §2] and [153]). The (scalar) vorticity field is approximated by 2-D delta-functions:

$$w = \sum_{\alpha} \Gamma_\alpha \delta(\boldsymbol{x} - \boldsymbol{x}_\alpha) \tag{7.4}$$

where α is the label of a point-vortex, Γ_α its strength, and $\boldsymbol{x}_\alpha$ its location. Since vortex deformation is zero for 2-D vortices, Γ_α is constant. The equations for these point-vortices can be written as a Hamiltonian system, in which the Hamiltonian is the total kinetic energy minus the so-called self-energy of the point-vortices. This subtraction of self-energy is necessary due to its infinity caused by the singularities in the velocity field at the locations of the point-vortices [10].

[9] These same restrictions had hindered Kelvin in his investigation of the vibrations of a "columnar vortex" [250]; see §5.3.4.

[10] Campbell in [32] has applied a vortex lattice to simulate point-vortex dynamics. In this method one also encounters the "problem" of self-energy of the vortices. However, he claims that self-energy does not affect the

Only recently the convergence of the point-vortex method for the 2-D incompressible Euler equation with smooth solutions has been proved (see e.g. [140]).

For 3-D flow simulations several vortex-point methods have been introduced.

One example of unsmoothed point-vortex methods is the one presented by Hou & Lowengrub [90]. In their set-up, vorticity is defined on a grid and a grid size is introduced. The displacement of the grid points is calculated from the rule of Biot-Savart. The Biot-Savart kernel is not regularized, since the authors show that for this method the kernel has a "natural cut-off" or vortex core. Vortex deformation is calculated by means of the Cauchy vorticity formula. Hou & Lowengrub claim to have proved the stability and convergence of this method.

Anderson & Greengard [8] have introduced two smoothed versions of the method of Hou & Lowengrub: one in which the Cauchy vorticity formula is retained and another one in which this formula has been replaced by the Helmholtz equation. For the former they have proved convergence. A detailed mathematical treatment of this method can be found in [70].

The grid-less variant of the Hou & Lowengrub method is the so-called vorton method as introduced by Novikov [168]. This 3-D method can be regarded as being closest to the 2-D point-vortex method. The essence of this method will be treated in Chapter 8, where we introduce our own (improved) vorton method. The second smoothed version as introduced by Anderson & Greengard has become known as the soft-vorton method, the smoothed version of Novikov's vorton method [11].

dynamics.

[11] The soft-vorton method is briefly discussed in Appendix B.

Chapter 8

The Vorton Method

8.1 Introduction

For the vortex methods mentioned in §7.3, several drawbacks have been mentioned. The most important ones will be repeated here.

For the use of any vortex element other than the unsmoothed vortex point, a drawback with regard to computational effort exists. Vortex methods involving vortex blobs (i.e. smoothed vortex-points) and (smoothed) vortex filaments often require a large amount of detailed information for the tracking of their location, strength, *and* vorticity distribution. Therefore, vortex points are preferable since they require less book-keeping.

With regard to the use of smoothed vortex elements, whether vortex points or vortex filaments, the somewhat arbitrary choice of the smoothing function has to be mentioned. It has become clear from literature that the numerical results also depend on this choice. Another characteristic of vortex methods using smoothed vortex elements is the requirement of overlap of the vortex elements, i.e. the distance between vortex elements has to be smaller than the sum of the characteristic dimensions of the smoothed vorticity distributions around them. According to Sarpkaya, in the overlap regions Helmholtz's First Theorem is not valid anymore and conservation of energy is violated [207, p.11].

Another important objection to all vortex-point methods mentioned in §7.3.3, is the fact that the vorticity field is not divergence-free in general (requirement 1 in the list of §7.2).

The vorton method is an unsmoothed vortex-point method according to the terminology introduced in §7.3. In this chapter the set-up of this method will be presented. Its original version, first elaborated by Novikov [1] [168] in 1983 and to be called the "original vorton

[1]Novikov has mentioned that his inspiration has partly come from the theory of superfluid vortices. Superfluidity has appeared to be one of the most successful applications of vorticity theory outside the field of classical fluid mechanics. In superfluid helium, a form of liquid helium that flows without viscosity or friction, very thin vortex filaments have been found experimentally with cores of atomic order of magnitude [48]. Researchers in this area have developed numerical simulation methods which show much resemblance to the vortex-filament method (see §7.3.1). Reconnection of these quantized vortices happens when distances between vortex lines are on atomic scales and thus involve quantum mechanics; it is claimed that on this scale there is no violation of Kelvin's Circulation Theorem (this suggests that also in inviscid flows reconnection might take place). However, in certain respects superfluid vortex motion is different from that in ordinary fluids. Vortex stretching does not take place, due to the quantization of circulation. Furthermore, at a given temperature and pressure a quantized vortex must always have the same core radius. The last few years, numerical studies of tangles of superfluid vortices have profited from the development of vortex methods in hydrodynamics [1].

Another vortex structure playing an important role in superfluids is the roton, a quantum-mechanical microscopic vortex ring. Brush [30] remarked, after a short discussion of Kelvin's work on vortex rings:

> ... a succesful investigation of the interaction of two vortex rings, in their modern reincarnation as rotons, would be an important contribution toward the synthesis of quantum mechanics and hydrodynamics, and toward the construction of a theory which promises to achieve a consistent and unambiguous deduction of observable properties from postulates about collective molecular motions, without attempting the apparently hopeless task of describing the motions of all the

method", may be regarded as the 3-D counterpart of 2-D point-vortex method (see §7.3.3), since it is based on a vorticity field consisting of 3-D delta-functions (compare (7.4)). These have been called "vortons" [2]. However, in 3-D flows we have to take into account the deformation of the vorticity field; this phenomenon is absent in 2-D flows.

Though the equations derived by Novikov for the displacement and deformation of vortons (the **vorton equations**) have appeared to provide the basis for seemingly correct simulations of vortex motion, it has also been realized that his derivation suffers from the fact that the vorticity field he applied is not divergence-free. This same weakness in Novikov's derivation causes the inconsistency between his vorton deformation equation and that derived by Kuwabara (see e.g. [114]). The only difference between these derivations is the choice of the basic equation: for Novikov this has been the Helmholtz equation (2.2), for Kuwabara it has been the so-called transposed representation of the Helmholtz equation.

To clarify the different representations of the Helmholtz equation and for convenience in our further elaboration in §8.3, we rewrite (2.2) as:

$$\frac{D\boldsymbol{w}}{Dt} = (\boldsymbol{v}') \circ \boldsymbol{w} \tag{8.1}$$

where the matrix $(\boldsymbol{v}')$ is defined by:

$$\begin{pmatrix} \frac{\partial v_1}{\partial x} & \frac{\partial v_1}{\partial y} & \frac{\partial v_1}{\partial z} \\ \frac{\partial v_2}{\partial x} & \frac{\partial v_2}{\partial y} & \frac{\partial v_2}{\partial z} \\ \frac{\partial v_3}{\partial x} & \frac{\partial v_3}{\partial y} & \frac{\partial v_3}{\partial z} \end{pmatrix} \tag{8.2}$$

where v_1, v_2, v_3 are the components of vector $\boldsymbol{v}$.

It can be shown that for vorticity fields satisfying relation (1.1) the Helmholtz equation (2.2), which in Cartesian coordinates reads:

$$\frac{Dw_i}{Dt} = \frac{\partial v_i}{\partial x_j} w_j \ ,$$

can be reformulated into the **transposed** representation of the Helmholtz equation:

$$\frac{Dw_i}{Dt} = \frac{\partial v_j}{\partial x_i} w_j$$

---

individual particles. The possibility of constructing such theories is of considerable significance for both physics and chemistry. [30, p.536]

Whereas, as discussed in §5.3.2, a fundamental critiscism of the vortex atom concerned its decrease of velocity with increasing energy, for the roton this is just the desired property!

Also in the related field of superconductivity, the vortex concept has gained a much-studied position. Recently, vortex analogies have also been found in lasers (see Weiss *et al.* in [33]).

For a popular account of superfluids, we refer to [48]; a text-book on both superfluidity and superconductivity is [263].

[2] The term "vorton" has been proposed in other areas of physics. In particle physics the vorton is defined as a stationary vortex ring, which can spin, have electric charge and behaves like a magnetic dipole. In many ways they are like ordinary particles, hence the name vorton in analogy with electron, photon, etc. Related to this quantum-scale vorton and based on its properties, "cosmic vortons" have been proposed. Generally, it is suggested that vortices, or cosmic strings, appear in a cosmological phase transition. During the period of the early universe, vorton-like structures which may even have extended over astronomical distances, could have been formed out of a Brownian network of vortices [45]. The name "vorton" has also been given to a monopole configuration with electromagnetic charge whose fields satisfy Maxwell's equations [61]. If such vortons should really exist as physical particles, "they would be quite different from presently known particles".

or

$$\frac{D\boldsymbol{w}}{Dt} = (\boldsymbol{v}')^* \circ \boldsymbol{w} \tag{8.3}$$

where $(\boldsymbol{v}')^*$ is the transposed of $(\boldsymbol{v}')$.

Consequently, a third formulation may be the **mixed** representation:

$$\frac{D\boldsymbol{w}}{Dt} = \frac{1}{2}[(\boldsymbol{v}') + (\boldsymbol{v}')^*] \circ \boldsymbol{w} \,. \tag{8.4}$$

Our derivation of the vorton deformation equation differs from Novikov's approach in two ways. First, it is based on a divergence-free vorticity field, which is an extension of Novikov's field; this is the subject of §8.2. Second, in §8.3 we apply a so-called weak formulation of the continuous equations from which the vorton equations are derived. This leads to a new vorton deformation equation and a proof that the inconsistency between Novikov's and Kuwabara's equations can only be removed by the use of a divergence-free vorticity field [3].

8.2 The Vorton Fields

In the original vorton method, the vorticity field is represented by:

$$\boldsymbol{w}(\boldsymbol{x},t) = \sum_{\alpha} \boldsymbol{\gamma}_\alpha(t)\ \delta(\boldsymbol{R}_\alpha(\boldsymbol{x},t)) \tag{8.5}$$

where $\boldsymbol{R}_\alpha(\boldsymbol{x},t) \equiv \boldsymbol{x} - \boldsymbol{r}_\alpha(t)$, $\delta(...)$ is the 3-D delta-function, and summation is over all vortons. The vortons are determined by a label α, a location vector $\boldsymbol{r}_\alpha$, and a strength vector $\boldsymbol{\gamma}_\alpha$ (which depends on time only).

The vector $\boldsymbol{\gamma}_\alpha$ has dimension of (volume/time) and can be regarded as a local vorticity distribution, given by:

$$\boldsymbol{\gamma}_\alpha \sim \int_{V_\alpha} \boldsymbol{w} \tag{8.6}$$

where the volume V_α around the location $\boldsymbol{r}_\alpha$ of vorton α gets infinitesimally small, while the integral remains finite.

From (8.5) Novikov derived the velocity field by applying the rule of Biot-Savart (2.3), giving:

$$\boldsymbol{v}(\boldsymbol{x},t) = \frac{1}{4\pi} \sum_{\alpha} \frac{\boldsymbol{\gamma}_\alpha \times \boldsymbol{R}_\alpha}{R_\alpha^3} \tag{8.7}$$

where $R_\alpha \equiv |\ \boldsymbol{R}_\alpha\ |$.

However, the field (8.5) is not divergence-free. Consequently, it does not satisfy one of the basic requirements of vortex methods (see §7.2) and consequently the rule of Biot-Savart may not be applied. In order to derive a divergence-free vorticity field, we have to take account of definition (1.1). The following procedure takes account of this requirement, while at the same time it provides a divergence-free velocity field and avoids application of the rule of Biot-Savart:

$$\text{vector potential } \boldsymbol{A} \quad \overset{\boldsymbol{v}=\nabla\times\boldsymbol{A}}{\Rightarrow} \quad \text{velocity } \boldsymbol{v} \quad \overset{\boldsymbol{w}=\nabla\times\boldsymbol{v}}{\Rightarrow} \quad \text{vorticity } \boldsymbol{w} \,.$$

[3] An alternative to the (original) vorton method is the soft-vorton method (already mentioned in §7.3.3) which is discussed in Appendix B.

For the vorton vector-potential field we take [4]:

$$\begin{aligned} \boldsymbol{A}(\boldsymbol{x},t) &= \frac{1}{4\pi}\sum_{\alpha}\frac{\boldsymbol{\gamma}_\alpha}{R_\alpha} \\ &= \sum_{\alpha}\phi(\boldsymbol{R}_\alpha)\,\boldsymbol{\gamma}_\alpha \end{aligned} \tag{8.8}$$

where we have introduced the function:

$$\phi(\boldsymbol{x}) \equiv \frac{1}{4\pi x}\,. \tag{8.9}$$

In mathematical terms ϕ is a Green's function, which is defined as the solution of the Poisson equation

$$\nabla^2\phi = -\delta(\boldsymbol{x})\,.$$

From this field we find the following velocity field:

$$\begin{aligned} \boldsymbol{v}(\boldsymbol{x},t) &= \sum_{\alpha}\boldsymbol{\nabla}\phi(\boldsymbol{R}_\alpha)\times\boldsymbol{\gamma}_\alpha \\ &= \frac{1}{4\pi}\sum_{\alpha}\frac{\boldsymbol{\gamma}_\alpha\times\boldsymbol{R}_\alpha}{R_\alpha^3} \end{aligned} \tag{8.10}$$

where $\boldsymbol{\nabla}\phi(\boldsymbol{R}_\alpha) \equiv (\boldsymbol{\nabla}\phi)|_{\boldsymbol{x}=\boldsymbol{R}_\alpha}$.

Finally, from (8.10) we get the following vorticity field by applying (1.1) [5]:

$$\begin{aligned} \boldsymbol{w}(\boldsymbol{x},t) &= \sum_{\alpha}\{\boldsymbol{\gamma}_\alpha\,\delta(\boldsymbol{R}_\alpha) + \phi''(\boldsymbol{R}_\alpha)\circ\boldsymbol{\gamma}_\alpha\} \\ &= \sum_{\alpha}\{\boldsymbol{\gamma}_\alpha\,\delta(\boldsymbol{R}_\alpha) + \boldsymbol{\nabla}[\boldsymbol{\nabla}\cdot(\phi(\boldsymbol{R}_\alpha)\boldsymbol{\gamma}_\alpha)]\} \\ &= \sum_{\alpha}\{\boldsymbol{\gamma}_\alpha\,\delta(\boldsymbol{R}_\alpha) - \frac{1}{4\pi}[\frac{\boldsymbol{\gamma}_\alpha}{R_\alpha^3} - \frac{3\boldsymbol{R}_\alpha(\boldsymbol{R}_\alpha\cdot\boldsymbol{\gamma}_\alpha)}{R_\alpha^5}]\} \end{aligned} \tag{8.11}$$

where

$$\phi''(\boldsymbol{R}_\alpha) \equiv \phi''|_{\boldsymbol{x}=\boldsymbol{R}_\alpha} \tag{8.12}$$

and the matrix ϕ'' is defined by:

$$\begin{pmatrix} \frac{\partial^2\phi}{\partial x\partial x} & \frac{\partial^2\phi}{\partial y\partial x} & \frac{\partial^2\phi}{\partial z\partial x} \\ \frac{\partial^2\phi}{\partial x\partial y} & \frac{\partial^2\phi}{\partial y\partial y} & \frac{\partial^2\phi}{\partial z\partial y} \\ \frac{\partial^2\phi}{\partial x\partial z} & \frac{\partial^2\phi}{\partial y\partial z} & \frac{\partial^2\phi}{\partial z\partial z} \end{pmatrix}. \tag{8.13}$$

Comparing this result to the original vorton field (8.5), we conclude that the second (gradient) part of (8.11), which is due to the the vector potential field not being divergence-free,

[4] The choice of the vector potential remains to be elucidated. We have chosen a function ϕ such that Novikov's velocity field (8.7) is obtained. If, for example, we require a divergence-free field $\boldsymbol{A}$, the choice of $\boldsymbol{A}$ (or ϕ) is restricted as explained in Appendix A. At the end of this Appendix we further discuss our vorton vector potential.

A more general treatment of (8.8), without determining function ϕ, can be found in Appendix B where the soft-vorton method is treated.

[5] This expression can also be found in Novikov's original paper [168].

renders the vorticity field divergence-free. It can be regarded as the nonlocal vorticity field surrounding the original singular vorton represented by the first part of (8.11). In a plane parallel to the strength vector and going through the location vector, the vortex lines of the nonlocal vorticity field resemble the "coil-like" streamline pattern of a doublet or dipole; see fig.8.1.

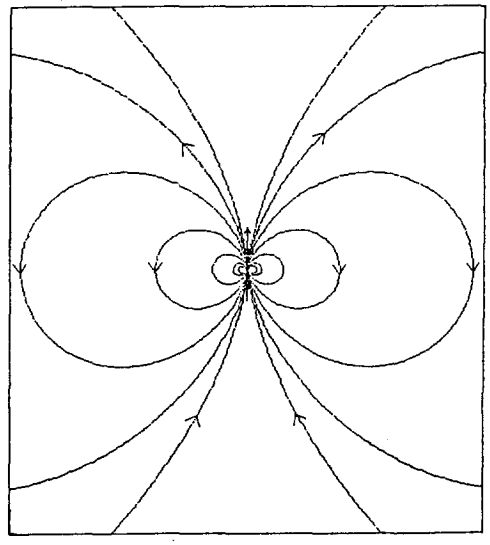

Figure 8.1: Vortex lines around one vorton (located at center, directed upwards).

Below, it will appear that this nonlocal part is crucial for a consistent derivation of the vorton deformation equation. Though it does not contribute to the integral of the rule of Biot-Savart (2.3), i.e. to the velocity field, it is of fundamental importance to a correct derivation of the vorton deformation equation, as will be shown below.

Mathematically speaking, the original vorticity field (8.5) has been projected onto a divergence-free field (8.11), without affecting the convolution with the Biot-Savart kernel.

8.3 The Vorton Equations

As indicated before, vorton dynamics consists of vorton displacement and vorton deformation. Below, the equations which describe both phenomena are presented; details of the derivation can be found in Appendix C. For the deformation equation, its superiority over Novikov's and Kuwabara's equations is discussed and an interpretation of our equation is attempted.

Derivation of the vorton displacement euqation is elementary. It follows directly from relation (7.1), which can be formulated here as:

$$\dot{\boldsymbol{r}}_\alpha = \tilde{\boldsymbol{v}}^\alpha(\boldsymbol{r}_\alpha, t) \tag{8.14}$$

where $\dot{\boldsymbol{r}}_\alpha \equiv d\boldsymbol{r}_\alpha/dt$ and the tilde indicates the field induced by all vortons except α [6].

[6]This suggests that "self-displacement" of vortons is eliminated. Justification for this elimination is given in the derivation presented in Appendix C.

Elaboration of (8.14), by applying (8.10), gives:

$$\dot{\boldsymbol{r}}_\alpha = \sum_{\beta \neq \alpha} \boldsymbol{\nabla}\phi(\boldsymbol{R}_{\alpha\beta}) \times \boldsymbol{\gamma}_\beta \tag{8.15}$$

where the function ϕ is given by (8.9) and $\boldsymbol{R}_{\alpha\beta} \equiv \boldsymbol{r}_\alpha - \boldsymbol{r}_\beta$.

With regard to vorton deformation, it is essential to remove the earlier mentioned inconsistency between the vorton deformation equations derived by Novikov and Kuwabara. We have devised a method for deriving vorton deformation equations from both representations of the Helmholtz equation which do not show any inconsistency. Its full details are revealed in Appendix C; below we give a short indication and the resulting equations.

We split the vorton velocity and vorticity fields derived in §8.2 into two parts. One part is the field induced by a vorton α for which we want to derive the deformation equation: velocity $\boldsymbol{v}^\alpha(\boldsymbol{x},t)$ and vorticity $\boldsymbol{w}^\alpha(\boldsymbol{x},t)$. The other part is the contribution from all other vortons, which is indicated by a tilde: $\tilde{\boldsymbol{v}}^\alpha(\boldsymbol{x},t)$ and $\tilde{\boldsymbol{w}}^\alpha(\boldsymbol{x},t)$.

The fundament of our approach is a weak formulation of the vortex deformation equations, i.e. these equations will be integrated about a small sphere B_α with radius ϵ and centred around the vorton location $\boldsymbol{r}_\alpha$. It is assumed that ϵ is so small that no other vorton locations are inside sphere B_α [7].

Using the splitting of the velocity and vorticity fields mentioned above, we get from (8.1) the following expression for the vorton deformation equation (in case of the Helmholtz equation):

$$\int_{B_\alpha} \frac{D(\boldsymbol{w}^\alpha + \tilde{\boldsymbol{w}}^\alpha)}{Dt} = \int_{B_\alpha} ((\boldsymbol{v}^\alpha + \tilde{\boldsymbol{v}}^\alpha)') \circ (\boldsymbol{w}^\alpha + \tilde{\boldsymbol{w}}^\alpha) \, . \tag{8.16}$$

Elaboration of expression (8.16) shows that the vorton deformation equation can be written as (see also (C.4) in Appendix C):

$$\dot{\boldsymbol{\gamma}}_\alpha = N_\alpha + S_\alpha \tag{8.17}$$

where

$$N_\alpha \equiv \sum_{\beta \neq \alpha} [\phi''(\boldsymbol{R}_{\alpha\beta}) \circ \boldsymbol{\gamma}_\alpha] \times \boldsymbol{\gamma}_\beta$$

and

$$S_\alpha \equiv \frac{1}{2} \sum_{\beta \neq \alpha} \boldsymbol{\gamma}_\alpha \times [\phi''(\boldsymbol{R}_{\alpha\beta}) \circ \boldsymbol{\gamma}_\beta] \tag{8.18}$$

where definition (8.12)has been used.

In the same way, from the transposed Helmholtz equation (8.3) one can derive (see also (C.6) in Appendix C):

$$\dot{\boldsymbol{\gamma}}_\alpha = K_\alpha - S_\alpha \tag{8.19}$$

where

$$K_\alpha \equiv \sum_{\beta \neq \alpha} \phi''(\boldsymbol{R}_{\alpha\beta}) \circ (\boldsymbol{\gamma}_\beta \times \boldsymbol{\gamma}_\alpha) \, .$$

Elaboration of (8.17) and (8.19) shows that both vorton deformation equations are equivalent, i.e. $N_\alpha + S_\alpha = K_\alpha - S_\alpha$.

[7] Note the resemblance of this approach to definition (7.3) of so-called weak solutions given in §7.2.

If we compare the deformation equations derived here with those found by Novikov [168] from the basic representation of the Helmholtz equation and by Kuwabara [114] from the transposed representation of the Helmholtz equation, we remark that Novikov's original vorton deformation equation is related to our expression N_α, i.e.:

$$\dot{\boldsymbol{\gamma}}_\alpha = N_\alpha \,. \tag{8.20}$$

This equation will be called the **N-equation.**

Kuwabara's vorton deformation equation is related to our expression K_α, i.e.:

$$\dot{\boldsymbol{\gamma}}_\alpha = K_\alpha \,. \tag{8.21}$$

This equation will be called the **K-equation.**

The inconsistency between Novikov's and Kuwabara's equations can now be stated as: $N_\alpha \neq K_\alpha$ Addition of the expression S_α to N_α and substraction of S_α from K_α causes complete equivalence. Remark that S_α is related to the nonlocal part of the vorton vorticity field (8.11), which explains why it is not present in the deformation equations derived by Novikov and by Kuwabara, who applied only the local field (8.5).

By adding equations (8.17) and (8.19), S_α disappears:

$$\dot{\boldsymbol{\gamma}}_\alpha = \frac{1}{2}\{N_\alpha + K_\alpha\} \,. \tag{8.22}$$

This will be called the **N+K-equation.**

Equation (8.22) suggests that S_α does not contribute to stretching of the vortons. This can be seen by taking the vector product of S_α (given by (8.18)) and $\boldsymbol{\gamma}_\alpha$.

Comparison of the expression (8.18) with the Euler equation for rigid body motion shows that S_α can be interpreted as a pure "spin" contribution. This can be demonstrated by regarding the rotation of a rigid body. For the angular momentum $\boldsymbol{M}$ of a rigid body we have:

$$\boldsymbol{M} = \boldsymbol{I} \circ \boldsymbol{\Omega}$$

where $\boldsymbol{I}$ is its inertia tensor and $\boldsymbol{\Omega}$ its angular velocity. Furthermore, for the rate of change of the angular momentum in time, we have:

$$\dot{\boldsymbol{M}} = \boldsymbol{M} \times \boldsymbol{\Omega} \,.$$

Combining these equations, we get:

$$\dot{\boldsymbol{M}} = \boldsymbol{M} \times (\boldsymbol{I}^{-1} \circ \boldsymbol{M}) \,.$$

Compare this expression with the vorton deformation due to S_α, i.e.

$$\dot{\boldsymbol{\gamma}}_\alpha = S_\alpha = \sum_{\beta \neq \alpha} \boldsymbol{\gamma}_\alpha \times [\phi''(\boldsymbol{R}_{\alpha\beta}) \circ \boldsymbol{\gamma}_\beta)] \,.$$

Some insight into expression (8.22) can be gained by observing that it can be rewritten as:

$$\dot{\boldsymbol{\gamma}}_\alpha = \frac{\partial G_\alpha}{\partial \boldsymbol{\gamma}_\alpha} \tag{8.23}$$

where

$$G_\alpha \equiv \frac{1}{2}\sum_{\beta\neq\alpha}[\phi''(\boldsymbol{R}_{\alpha\beta})\circ\boldsymbol{\gamma}_\alpha]\cdot(\boldsymbol{\gamma}_\beta\times\boldsymbol{\gamma}_\alpha)\,. \tag{8.24}$$

In its turn, expression (8.24) may be rewritten as:

$$G_\alpha = \frac{\partial H_\alpha}{\partial \boldsymbol{r}_\alpha}\cdot\boldsymbol{\gamma}_\alpha \tag{8.25}$$

where

$$H_\alpha \equiv \frac{1}{2}\sum_{\beta\neq\alpha}\boldsymbol{\gamma}_\alpha\cdot\boldsymbol{v}^\beta(\boldsymbol{r}_\alpha)\,.$$

H_α may be called the local helicity density, defined as the integrand of total helicity (see §C of the Interlude). Apparently, the deformation of vorton α is related to the change of helicity density at its location caused by all vortons $\beta\neq\alpha$, due to the movement of vorton α in the direction of its strength vector $\boldsymbol{\gamma}_\alpha$.

From (8.23) and (8.25) we derive:

$$\dot{\boldsymbol{\gamma}}_\alpha = \frac{\partial}{\partial\boldsymbol{\gamma}_\alpha}\{\frac{\partial H_\alpha}{\partial\boldsymbol{r}_\alpha}\cdot\boldsymbol{\gamma}_\alpha\}$$

from which follows:

$$\dot{\boldsymbol{\gamma}}_\alpha = (\frac{\partial}{\partial\boldsymbol{\gamma}_\alpha}\{\frac{\partial H_\alpha}{\partial\boldsymbol{r}_\alpha}\})^*\circ\boldsymbol{\gamma}_\alpha + \frac{\partial H_\alpha}{\partial\boldsymbol{r}_\alpha}\,. \tag{8.26}$$

Comparison with (8.22) shows the first part of (8.26) to be equal to $\frac{1}{2}N_\alpha$ while the second part is equal to $\frac{1}{2}K_\alpha$ [8].

Since G_α (8.24) is homogeneous of second degree in $\boldsymbol{\gamma}_\alpha$, we find the following expression for the stretching of vorton α:

$$\frac{d\gamma_\alpha^2}{dt} = 4G_\alpha\,.$$

We conclude that levels of constant stretching of vorton α are equal to levels of constant G_α.

To investigate these levels of constant nonzero vorton stretching, we regard the configuration of two vortons, 1 and 2. Without violating generality, we take

$$\boldsymbol{r}_1 = \begin{pmatrix}0\\0\\0\end{pmatrix},\ \boldsymbol{\gamma}_1 = \begin{pmatrix}0\\0\\1\end{pmatrix},\ \boldsymbol{r}_2 = \begin{pmatrix}x\\y\\z\end{pmatrix},\ \boldsymbol{\gamma}_2 = \begin{pmatrix}0\\1\\0\end{pmatrix}\,.$$

We investigate levels on which vorton 2 has constant stretching due to vorton 1. From (8.24) we find surfaces given by $x\,y = C\,(x^2+y^2+z^2)^{5/2}$, where C is a constant. In fig.8.2, the surface for $C=1$ has been drawn. We see that the area of influence of vorton 1 is symmetrical around its strength vector. The four "lobes" are separated by the zero-stretching surfaces $G_2=0$, which in this case are given by $x=0$ and $y=0$. Two oppositely placed lobs have the same stretching levels, of either positive or negative value.

[8] This last result has also been derived by Kuwabara (see e.g. [114]).

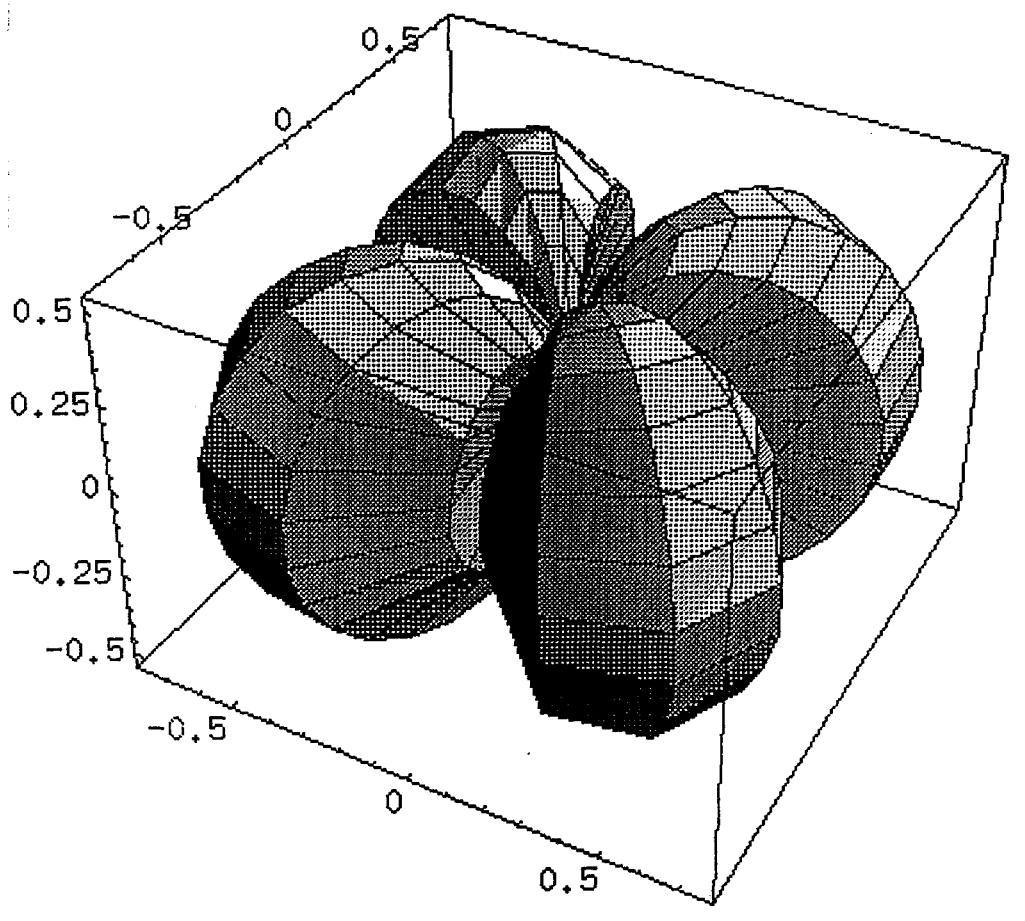

Figure 8.2: Surface given by $xy = (x^2 + y^2 + z^2)^{5/2}$, illustrating the influence of vorton 1 on vorton 2 (see text).

Chapter 9

Numerical Simulations: Preparatory Remarks

The vorton equations, presented in §8.3, will be used to simulate the dynamics of continuous vortex structures. This is done by constructing a discrete vorton representation of these structures and solving the vorton equations by means of a numerical scheme. Comparison of the numerical results with results from other numerical simulations and from experiments will clarify the applicability of the vorton method. More specifically, the simulation will provide information on the fulfilment of requirements 2 (correct modelling of continuous distributions of vorticity), 3 (correct representation of deformation and interaction of vortex structures), 4 (conservation of motion-invariants), and 5 (no negative effects of remeshing) as posed in §7.2. If we find a satisfactory performance of our vorton method and agreement with results found by others, confidence in the applicability of the method to other, more complicated, flow phenomena, will be established.

In the last decade, several vorton simulations have been reported in literature in which both the N-equation (8.20) and the K-equation (8.21) have been used. We mention those by Novikov in [168] and [170]; by Novikov *et al.* in [6]; by Novikov and Aksman in [5]; and by Kuwabara in e.g. [113] and [114].

Besides, at least two dissertations have been (partly) devoted to the vorton method and its application to numerical simulations. Pedrizzetti [178] applied the N-equation [1], while Winckelmans [283] studied both the N-, K-, and N+K-equations and also regarded the soft-vorton method (see Appendix B) and the possibility of adding viscous diffusion to the vorton equations [2].

In Chapter 10, we will present the results of the numerical simulations of several test cases. In this preparatory chapter, we discuss the choice of these cases and their relation to the aim of our research (§9.1); we give some details of the numerics (§9.2); we introduce the so-called diagnostics which are used in our evaluation of the numerical results (§9.3); and we describe the technique of vorton division whose applicability and value will be investigated by means of some of the simulations of Chapter 10 (§9.4).

9.1 Aims and Choices

The choice of the test cases which have been regarded and the choice of the characteristics and diagnostics calculated for these cases have been directed by the following considerations (compare some of the requirements mentioned in §7.2):

[1] Note that Pedrizzetti has added a "divergence filtering procedure". Apparently, this seemed to him the only way to ascertain reasonable results from his simulations, despite the non-divergence-free vorticity field. This procedure tends to align the vorton strength vectors $\boldsymbol{\gamma}$ with the local vector $\nabla \times \boldsymbol{v}$. However, he admitted that the filtering has "no clear physical meaning" [177].

[2] Winckelmans has applied a technique called "relaxation of the vorticity divergence" to ensure a (almost) divergence-free vorticity field. This technique requires the solving of a system of linear equations. However, it appears that these equations act dissipatively.

- **availability of experimental, numerical, or analytical data**

  Only when comparison of the simulation results with the same kind of data obtained by others is possible, an evaluation of our vorton method (i.e. application of the N+K-equation) and its applicability can be made. We realize that experimental data always relate to viscous vortex structures, and that the influence of viscosity may not always be disregarded.

- **possibility of the representation of elementary vortex phenomena**

  Among the many phenomena related to vortex motion, we have tried to find test cases which, in a generic way, allow the study of vorticity deformation (stretching), vortex core deformation, vortex reconnection, and alignment of anti-parallel vortex tubes (see §C of the Interlude).

- **possibility of the imposition of boundary conditions**

  In case of the vorton method the possibilities to impose boundary conditions are limited. As has already been indicated by Novikov [169], only the free-slip boundary condition can be realized. This can be done by adding so-called mirrored vortons, similar to the situation sketched in fig.7.1. For the simulation of non-closed infinite vortex filaments periodic boundary conditions should be imposed, requiring a substantial extra amount of computational effort. We have restricted the simulations primarily to (elliptical) vortex ring in 3-D unbounded space or near a planar free-slip boundary.

The two main aims of our numerical research have been to:

- investigate the characteristics of the vorton method introduced in Chapter 8 (i.e. the N+K-equation (8.22) for the vorton deformation): its possible applications, its limitations with regard to simulation of flow phenomena, and its satisfaction of the vortex method requirements as mentioned in §7.2;

- compare the simulations obtained from applying both the N-, the K-, and the N+K-equation; though we have shown in §8.3 by means of theoretical arguments that the last one is to be preferred, we will find confirmation of this claim by means of the numerical results.

All test cases chosen for our numerical simulations involve the interaction of vortex rings. Several reasons exist to concentrate on this vortex structure:

- As indicated in the vortex-atom-part and the Interlude, the vortex ring has been the subject of long-standing research into several of its aspects. Today it is still one of the most studied vortex structures.

- Furthermore, a vortex ring may be characterized by only a few quantities, i.e. the ring radius R, the number of vortons N, and the circulation Γ; see fig.2.3 [3].

- A vorton representation of the vortex ring is relatively easy: the vorton locations $\boldsymbol{r}_\alpha$ are put at equal distances on a circle of radius R, and the vorton strength vectors $\boldsymbol{\gamma}_\alpha$ - all of the same modulus γ - are tangential to this circle; see fig.9.1 [4].

[3] However, as the reader may already realize, real vortex rings are also characterized by a distribution of vorticity in the ring's core.

[4] Other representations of vortex rings by means of vortons can be imagined. One example is shown in fig.10.28 in §10.4.2. Alternatives like these will not be investigated in this thesis, but we will return to their

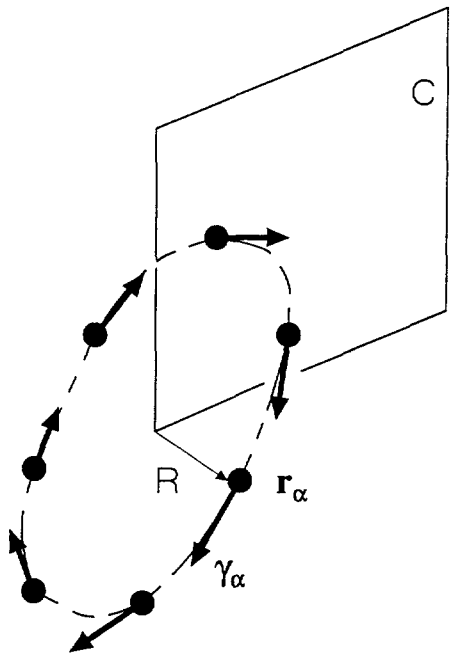

Figure 9.1: A vorton ring; vortons are indicated by arrows. (Curve C is related to calculation of the ring's circulation.)

- Despite their simple appearance, the interaction of vortex rings is far from simple and trivial and shows the elementary vortex phenomena which we want to study (see above).
- Vortex rings are closed structures, requiring no special attention with regard to boundary conditions in the numerical simulations as in case of (infinite) vortex filaments (see above).
- Finally, vortex rings have been proposed as candidates for the role of coherent structures in turbulence (see §B of the Interlude and §10.6). Therefore, knowledge on their behaviour may increase our understanding of turbulent phenomena.

The following six test cases have been chosen, the essence of which will shortly be explained here:

- **single vorton ring**

  Before regarding the interaction of several circular vorton rings or the behaviour of a single noncircular vorton "ring", one should get an impression of the characteristics (e.g. its core) and the behaviour of a single circular vorton ring (e.g. stability). Since a single circular vortex ring will not exhibit deformation without influences from other vortex structures or boundaries, the simulation results for this case will not depend on the vorton equations applied and consequently no comparison has been made between the three different vorton equations.

possible significance in Chapter 11.

- **single pseudo-elliptical vortex ring**

  The simplest variation on the circular vorton ring is an elliptically shaped "ring". For reasons of convenience we only regard the so-called pseudo-elliptical vorton ring (see fig.10.7). Contrary to the circular ring, an elliptical ring will deform during translation; therefore, it forms a test case for the three different vorton equations. It turns out that the behaviour of this ring depends on the aspect ratio of the ellipse and can involve reconnection. Therefore, it is a good test case for the simulation of this last phenomenon.

- **head-on collision of two coaxial vorton rings**

  This configuration consists of two identical circular vortex rings which approach each other along a common axis. It is especially attractive since it has been treated analytically (though only for Kelvin-rings; see §A.2 of the Interlude). Besides, it is suited for the study of core deformation during close approach of vortex tubes.

- **oblique interaction of two initially parallel vortex rings**

  This configuration is one of the most elementary test cases showing the phenomenon of vortex reconnection. Besides, it is one of the few which can be compared rather extensively with experimental results.

- **interaction of two knotted vortex rings**

  This configuration, though unfortunately it cannot be studied experimentally, is one of the most elementary test cases to investigate the phenomenon of vortex alignment.

- **single vorton ring in a shear flow above a flat plate**

  This configuration is chosen to increase our insight into the behaviour of coherent structures in a boundary layer. Though the model may be too simple to describe all aspects of coherent structures, at least it shows the applicability of the vorton method in this kind of research and the influence of shear flow and (free-slip) walls.

9.2 Details of the Numerical Simulations

In most of the simulations to be presented in the next section, a so-called **standard vorton ring** has been used. The standard vorton ring is characterized by circulation $\Gamma = 820\ cm^2/s$ and radius $R = 0.8\ cm$.

All simulations have been carried out on an HP9000 835 minicomputer. Unless otherwise stated, the N+K-equation (8.22) has been used. To solve the vorton equations, which are ordinary differential equations, use has been made of a 4th order Runge-Kutta method.

The time step Δt has been adapted constantly during the simulation to a value given by R_{min}^3/γ_{max}: $\Delta t = CR_{min}^3/\gamma_{max}$ (C is constant). R_{min} is the minimum distance between any two vortons [5] and γ_{max} is the maximum vorton strength of the two vortons between which R_{min} occurs: $\gamma_{max} = \max(\gamma_1, \gamma_2)$. See fig.9.2. This procedure is based on the following consideration: if we consider vorton 2 of this pair of vortons as a passive particle, we find from the vorton displacement equation (8.15) that it will turn around vorton 1 in a time proportional to the expression mentioned above. The proportionality factor C used in our simulations has been of

[5] This minimum distance R_{min} only concerns the distances between vortons not belonging to the same vortex structure, i.e. not in the same vorton ring. This time step adaptation procedure has not been applied in case of the pseudo-elliptical vorton ring.

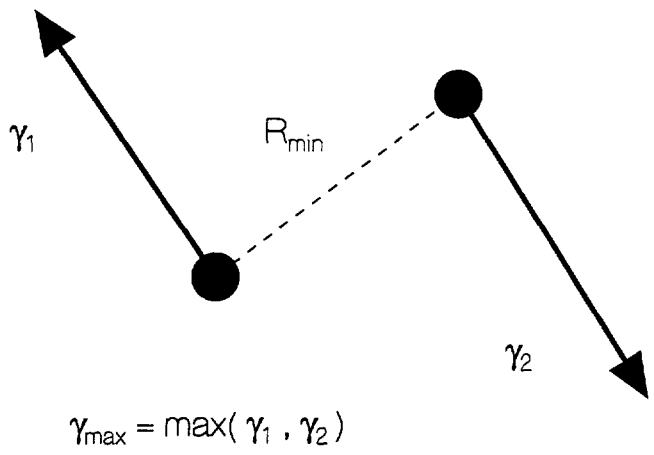

Figure 9.2: The vorton configuration on which time-step adaptation is based (see text).

order 1. A maximum time step Δt_{max} was imposed, usually $10^{-4}s$. Both values are based on experience obtained during the performance of the simulations.

Unless otherwise stated, all length scales are in cm, and all time scales in s.

9.3 Diagnostics

Our numerical study of vortex phenomena consists of considering the general, qualitative behaviour of the simulated test cases and comparing it with experimental results. Besides, an investigation will be done regarding some flow diagnostics, i.e. quantitative data which can be visualized either by means of graphs or data visualization packages.

In general, diagnostics can serve three purposes:

1. they may be indicators of the accuracy of the numerical simulations;
2. they may be useful in the comparison of different simulation methods;
3. they may be useful in the comparison of results from simulations with those from experiments.

For our simulations we introduce two kinds of diagnostics: motion-invariants and fields. The first serves the purposes 1 and 2 mentioned above. The second one is meant to serve purpose 3. By means of these diagnostics, we get insight into the behaviour of the cases studied, into the applicability of the proposed vorton method, and into the latter's performance as compared to Novikov's and Kuwabara's vorton method (see §8.3).

9.3.1 Motion-Invariants

As for any vortex method, for the vorton method an investigation into the conservation of so-called motion-invariants may be an important test of its accuracy (see §7.2).

In any infinite, inviscid, 3-D flow the following motion-invariants have to be conserved by the flow [6]:

[6]The existence of motion-invariants and their expressions in fluid mechanics can be derived by representing

- **total vorticity:**

$$\boldsymbol{\Omega} \equiv \int_V \boldsymbol{w} \, .$$

$\boldsymbol{\Omega}$ is always conserved for flows with a velocity field approaching zero at infinity at an appropriate rate, since

$$\int_V \boldsymbol{w} = \int_{\partial V} \boldsymbol{v} \times \boldsymbol{n}$$

where ∂V is the (infinitely distant) boundary of volume V.

For the original vorton vorticity field (8.5), we get the simple result:

$$\boldsymbol{\Omega} = \sum_\alpha \boldsymbol{\gamma}_\alpha \, . \tag{9.1}$$

For the divergence-free vorton vorticity field (8.11), the integral related to $\boldsymbol{\Omega}$ is not defined due to the singular nonlocal part. However, Appendix C shows that for a volume V equal to a small sphere around a vorton location $\boldsymbol{r}_\alpha$, Ω is proportional to γ_α. This may suggest that (9.1) remains valid for our vorton method.

However, expression (9.1) is easily shown to be an inappropriate expression for $\boldsymbol{\Omega}$. It can only be conserved if the expression for $\dot{\boldsymbol{\gamma}}_\alpha$ is pairwise anti-symmetric for any pair of vortons α and β. This is only the case for the K-equation (8.21), but not so for the N-equation (8.20) and the N+K-equation (8.22). This shows that our assumption on the validity of (9.1) is not valid. Consequently, we have decided to disregard (9.1) as a motion-invariant.

- **total linear momentum:**

$$\boldsymbol{P} \equiv \int \boldsymbol{v} \, . \tag{9.2}$$

Due to the singular behaviour of the vorton velocity field (8.10) an expression for $\boldsymbol{P}$ cannot be obtained for the integral in expression (9.2).

Expression (9.2) can be rewritten into the form of the so-called Kelvin impulse [7] (see (A.3) in Appendix A):

$$\boldsymbol{P} \equiv \frac{1}{2} \int_V \boldsymbol{x} \times \boldsymbol{w} \tag{9.3}$$

if the vorticity field satisfies the condition

$$| \, \boldsymbol{w}(\boldsymbol{x}) \, | \sim x^{-n} \, , \; n > 3 \;\; \text{as} \;\; x \to \infty \tag{9.4}$$

is satisfied. This condition is not fulfilled by our vorton vorticity field (8.11). If instead we apply the original vorticity field (8.5) to (9.3), we get:

$$\boldsymbol{P} = \frac{1}{2} \sum_\alpha \boldsymbol{r}_\alpha \times \boldsymbol{\gamma}_\alpha \, . \tag{9.5}$$

---

the Euler or Helmholtz equation in terms of so-called Poisson brackets, related to Lie-algebra (see e.g. [72]).

However, for of a divergence-free vector potential the existence of the first three motion-invariants mentioned below can directly be derived as shown in Appendix A. Though our field (8.8) is not divergence-free, the results provided in Appendix A explain some of the problems in the derivation of motion-invariants given below.

[7] This denomination seems historically incorrect, since this expression has not been traced in Kelvin's work. It has been derived by J.J. Thomson in his *Treatise* (see §5.1).

Since expression (9.1) is unequal to zero, (9.5) shows lack of invariance with regard to the location of the frame of reference. Nevertheless, it will be taken as representation of $\boldsymbol{P}$ in the simulations presented in Chapter 10.

- **total angular momentum:**

$$\boldsymbol{J} \equiv \int_V \boldsymbol{x} \times \boldsymbol{v} \, . \tag{9.6}$$

As for linear momentum, no expression for $\boldsymbol{J}$ can be derived from expression (9.6) due to the singular behaviour of the vorton velocity field (8.10).

Under the same condition (9.4) as mentioned above for $\boldsymbol{P}$, we find (compare (A.5) in Appendix A):

$$\boldsymbol{J} = \frac{1}{3} \int_V \boldsymbol{x} \times (\boldsymbol{x} \times \boldsymbol{w}) \, . \tag{9.7}$$

As for linear momentum, our expression to be used as diagnostic for total angular momentum is derived by applying the original vorton vorticity field (8.5) to (9.7):

$$\boldsymbol{J} = \frac{1}{3} \sum_\alpha \boldsymbol{r}_\alpha \times (\boldsymbol{r}_\alpha \times \boldsymbol{\gamma}_\alpha) \, . \tag{9.8}$$

- **total kinetic energy:**

$$E \equiv \int_V \boldsymbol{v} \cdot \boldsymbol{v} \, . \tag{9.9}$$

Direct calculation of E by substituting the vorton velocity field (8.10) into (9.9) can be achieved (see [283]) if the so-called self-energy E_0 of the vortons is subtracted (compare with the case of 2-D point-vortices; see §7.3.1), which in the final result is indicated by the omission of terms $\alpha = \beta$. The remaining part of E is called the interaction-energy E_i:

$$E_i = \frac{1}{8\pi} \sum_{\alpha \neq \beta} \{ \frac{\boldsymbol{\gamma}_\alpha \cdot \boldsymbol{\gamma}_\beta}{R_{\alpha\beta}} + \frac{(\boldsymbol{\gamma}_\alpha \cdot \boldsymbol{R}_{\alpha\beta})(\boldsymbol{\gamma}_\beta \cdot \boldsymbol{R}_{\alpha\beta})}{R^3_{\alpha\beta}} \} \, . \tag{9.10}$$

The same result can be derived by a different approach, which makes use of an expression for the energy spectrum $E(k)$ [8]. The energy spectrum also consists of a self-energy part and an interaction-energy part [9]:

$$E(k) = E_0(k) + E_i(k) \tag{9.11}$$

where

$$E_0(k) = \frac{1}{6\pi^2} \sum_\alpha \boldsymbol{\gamma}_\alpha \cdot \boldsymbol{\gamma}_\alpha \tag{9.12}$$

$$E_i(k) = \frac{1}{4\pi^2} \sum_{\alpha \neq \beta} \{ \phi_1(kR_{\alpha\beta})(\boldsymbol{\gamma}_\alpha \cdot \boldsymbol{\gamma}_\beta) + \frac{\phi_2(kR_{\alpha\beta})(\boldsymbol{\gamma}_\alpha \cdot \boldsymbol{R}_{\alpha\beta})\,(\boldsymbol{\gamma}_\beta \cdot \boldsymbol{R}_{\alpha\beta})}{R^2_{\alpha\beta}} \} \tag{9.13}$$

[8] For details we refer to [6].

[9] This spectrum can be obtained from that for soft vortons derived by Kiya and Ishii in [105] by taking $\sigma \to 0$ (see Appendix B).

where

$$\phi_1(z) \equiv \frac{(z^2-1)\sin z + z\cos z}{z^3}$$
$$\phi_2(z) \equiv \frac{(3-z^2)\sin z - 3z\cos z}{z^3}.$$

Integration of $E(k)$ over all wave numbers k ranging from 0 to ∞ again shows that total kinetic energy is only finite if the self-energy E_0 is subtracted.

To have a possible indication of the behaviour of E_0, we take as a diagnostic:

$$E_0 = \sum_\alpha \gamma_\alpha^2 \tag{9.14}$$

which is based on the self-energy spectrum $E_0(k)$ given by (9.12).

- **total helicity**:

$$H \equiv \int_V \boldsymbol{v}\cdot\boldsymbol{w}\,. \tag{9.15}$$

As discussed in §C of the Interlude, helicity is related to the topology of vortex structures in a flow (see e.g. [161]). Besides, H is a fundamental motion-invariant of inviscid flows.

For the integral (9.15) to be convergent, it is sufficient that the vorticity field $|\,\boldsymbol{w}(\boldsymbol{x})\,| \sim x^{-4}$ as $x \to \infty$ for a fluid of infinite extent, in order to ensure invariance of H [157]. The vorton vorticity field (8.11) does noy satisfy this requirement.

However, the above condition is not a *necessary* one and an expression for H can be derived from our vorton fields without objections. As for total kinetic energy, helicity has to be split into a self-helicity part and an interaction-helicity part. Inserting the vorton velocity (8.10) and vorticity (8.11) fields in (9.15), we get for the interaction-helicity:

$$H_i = \frac{1}{4\pi}\sum_{\alpha,\beta} \frac{\boldsymbol{R}_{\alpha\beta}\cdot(\boldsymbol{\gamma}_\alpha \times \boldsymbol{\gamma}_\beta)}{R_{\alpha\beta}^3}\,. \tag{9.16}$$

Though not a motion-invariant in the same sense as those listed above, we also have to regard the diagnostic provided by the circulation Γ. In §4.1 Kelvin's derivation of the circulation concept (4.2) and its most important property, the circulation theorem, were presented. From this theorem it follows that, as for a vortex ring, the circulation of a vorton ring should be conserved.

To calculate a value for Γ for the vorton ring, a closed curve C will be chosen as indicated in fig.9.1 along which the velocity field (8.10) will be integrated. This will be done by taking the value of the tangential velocity component at equally spaced grid points along the curve, multiplying this value by the local distance between the points, and adding all contributions.

Novikov [168] has shown analytically that in the limit of infinite number of vortons, i.e. $N \to \infty$, the circulation of a vorton ring of radius R can be written as:

$$\Gamma = \frac{\gamma}{\frac{2\pi R}{N}} \tag{9.17}$$

where γ is the strength of each vorton in the ring and the denominator can be regarded as the distance between the vortons in the ring. Despite the relatively small values for N in our

simulations, expression (9.17) has been used in the numerical simulations to obtain the value of the vorton strength γ for the vortons in a vorton ring of given radius R, circulation Γ, and number of vortons N.

9.3.2 Fields

The following fields will be regarded:

- velocity field

  The velocity field $\boldsymbol{v}$ is given by expression (8.10).

- vorticity field

  The vorticity field used as a diagnostic is the nonlocal gradient part of the divergence-free vorton vorticity field (8.11). To stress the point that this field is only part of the divergence-free vorticity field (8.11), it will be indicated by $\bar{\boldsymbol{w}}$, i.e.:

$$\bar{\boldsymbol{w}}(\boldsymbol{x},t) \equiv \sum_{\alpha} \boldsymbol{\nabla}(\boldsymbol{\nabla} \cdot \frac{\boldsymbol{\gamma}_\alpha}{R_\alpha}) \,. \tag{9.18}$$

The fields are calculated on the points of a rectangular grid which is constantly adapted to the vorton configuration. Due to computational restrictions the grid is usually limited to 40^3 grid points.

Notice that both fields show singular behaviour at the vorton locations. To avoid problems coincidence of the grid points with vorton locations has been prohibited by either shifting the grid or nelgecting the contribution of some vortons during the calculation of the fields.

Visualization of the vorticity field, by means of isosurfaces of its magnitude $|\,\bar{\boldsymbol{w}}\,|$, has been done by means of the graphics package AVS. Some figures show the vortons themselves (as arrows, consisting of a line and a open circle as arrow head). These have been made by means of the specially-written package Vectrix. In these pictures the vorton strength vectors have been scaled to the same length.

9.4 Vorton Division

One of the seemingly attractive properties of the vorton method is the possibility of adding and removing vortons. The addition of vortons, to be called vorton division, has been introduced by Kuwabara (see e.g. [113]) and also has been applied by Pedrizetti [178] and Winckelmans [283].

Its principle is illustrated in fig.9.3: if the distance $\Delta x = \Delta x_1 + \Delta x_2$ of a vorton α to its two nearest neighbours has increased beyond a certain value λ times the original distance Δx_0, vorton division will be imposed [10].

For the authors mentioned above, division meant the removal of vorton α and addition of two new vortons at locations $\pm(\Delta x/8)\ \boldsymbol{\gamma}_\alpha/\gamma_\alpha$. In several cases this procedure will lead to an irregular distribution of vortons in azimuthal direction, e.g. in the case of a radially growing vorton ring (as we will encounter in §10.3). Therefore, we have adopted another vorton division procedure: two new vortons will be added in between vorton α and its neighbours, while vorton α is left untouched; see fig.9.3(b).

Various options could be proposed for assigning vorton strengths to the added vortons and for optional updating of the strengths of the existing vortons. The simplest choice is to

[10] Discussion of the value to be given to λ will be postponed to §10.3.2.

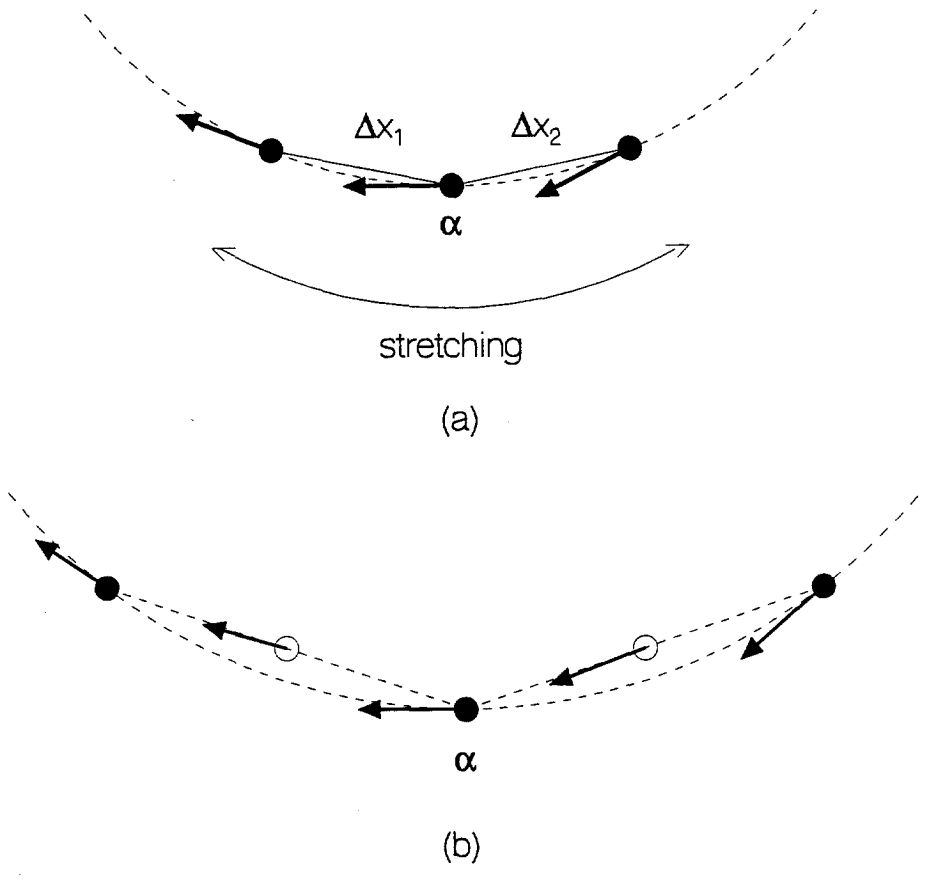

Figure 9.3: Illustration of the vorton division procedure (see text): (a) before ($\Delta x_0 = \Delta x(t=0) = \Delta x_1 + \Delta x_2$) and (b) after division ($\Delta x = \lambda \Delta x_0$). Added vortons are indicated by open dots.

take for the strength of each added vorton the mean value of its two neighbours in the ring and to omit updating of the existing vortons. However, in that case no attention has been given to the influence of vorton division on the conservation of the expressions for the motion-invariants mentioned in §9.3.1. Our choice of updating the vortons after division is based on the conservation of circulation [11] as defined by (9.17). This means that for every vorton the quantity

$$\frac{\gamma}{\Delta x} \tag{9.19}$$

is to be conserved, where γ is its strength and Δx is defined in fig.9.3(a). This procedure will be called "division with updating".

Summarizing, our division procedure is as follows:

1. new vortons are added as indicated in fig.9.3 whenever Δx becomes larger than $\lambda \Delta x_0$;

[11] Winckelmans [283, §3.5.7] has suggested that division procedures can be set up which conserve both linear momentum as given by expression (9.5) and angular momentum given by (9.8). However, two remarks have to be made. First, we have indicated in §9.3.2 that these expressions cannot be proper motion-invariants in case of the vorton method as applied here. Secondly, one could wonder whether conservation of both these invariants assures the conservation of other motion-invariants.

2. the strengths of the existing vortons are updated such that the value of expression (9.19) becomes equal to the value it had just before the division started;

3. the newly added vortons get strengths which are the average of the strengths of their two neighbours;

4. the former values of Δx_0 are updated according to the new distances between the vortons.